REPORT DOCUMENTATION PAGE

Form Approved
OMB No. 0704-0188

PLEASE DO NOT RETURN YOUR FORM TO THE ABOVE ORGANIZATION.

1. REPORT DATE *(DD-MM-YYYY)*	2. REPORT TYPE	3. DATES COVERED *(From - To)*
29-11-2011	Final	09/01/2008 - 08/31/2011

4. TITLE AND SUBTITLE
Diode lasers and light emitting diodes operating at room temperature with wavelengths above 3μm

5a. CONTRACT NUMBER
FA9550-08-1-0458

5b. GRANT NUMBER

5c. PROGRAM ELEMENT NUMBER

6. AUTHOR(S)
Gregory Belenky, Leon Shterengas, Dmitry Donetsky, Sergey Suchalkin

5d. PROJECT NUMBER

5e. TASK NUMBER

5f. WORK UNIT NUMBER

7. PERFORMING ORGANIZATION NAME(S) AND ADDRESS(ES)
State University of New York at Stony Brook,
Department of ECE, SUNY at Stony Brook, Stony Brook, NY 11794-2350

8. PERFORMING ORGANIZATION REPORT NUMBER

9. SPONSORING/MONITORING AGENCY NAME(S) AND ADDRESS(ES)
US Air Force Office of Scientific Research
875 N. Randolph St.
Suite 325
Arlington, VA 22203

10. SPONSOR/MONITOR'S ACRONYM(S)

11. SPONSOR/MONITOR'S REPORT NUMBER(S)
AFRL-OSR-VA-TR-2012-0289

12. DISTRIBUTION/AVAILABILITY STATEMENT
A - Approved for public release

13. SUPPLEMENTARY NOTES

14. ABSTRACT
New family of the GaSb-based type-I quantum well (QW) diode lasers and light emitting diodes (LED) were designed and fabricated. World record parameters were demonstrated for all devices. Diode laser operate in continuous wave (CW) regime at room temperature (RT) up to 3.4 μm. More than 350 mW of CW power was demonstrated for 3 μm emitting multimode lasers. Single spatial mode 3 – 3.2 μm diode lasers were developed. LEDs operate at wavelength above 4 μm at RT. Dual color mid-infrared LEDs were designed and fabricated. Metamorphic diode lasers grown onto GaSb substrates using compositionally graded buffers were designed and fabricated.

15. SUBJECT TERMS
GaSb, Type-I QW, diode lasers, light emitting diodes, high power, mid-infrared, single spatial mode, ridge waveguide, metamorphic molecular beam epitaxy

16. SECURITY CLASSIFICATION OF:			17. LIMITATION OF ABSTRACT	18. NUMBER OF PAGES	19a. NAME OF RESPONSIBLE PERSON
a. REPORT	b. ABSTRACT	c. THIS PAGE			Leon Shterengas
U	U	U	UU	20	19b. TELEPHONE NUMBER *(Include area code)* 631-632-9376

Reset

Final Report

Contract FA9550-08-1-0458,

Diode Lasers and Light Emitting Diodes Operating at Room Temperature with Wavelengths Above 3μm

New family of the GaSb-based type-I quantum well (QW) diode lasers and light emitting diodes (LED) were designed and fabricated. World record parameters were demonstrated for all devices. Diode laser operate in continuous wave (CW) regime at room temperature (RT) up to 3.4 μm. More than 350 mW of CW power was demonstrated for 3 μm emitting multimode lasers. Single spatial mode 3 – 3.2 μm diode lasers were developed. LEDs operate at wavelength above 4 μm at RT. Dual color mid-infrared LEDs were designed and fabricated. Metamorphic diode lasers grown onto GaSb substrates using compositionally graded buffers were designed and fabricated.

The report contained three parts: (a) development of the multimode diode lasers; (b) design and technology of metamorphic Sb-based diode lasers; (c) development of single spatial mode ridge lasers; and (d) development of LEDs.

(a). Multimode 3 – 3.4 μm diode lasers.

Diode lasers operating in the spectral region above 3 μm are required for a variety of applications. Many important gases and other chemical agents can be remotely detected by tunable laser spectroscopy in this spectral region. For instance, methane, ethane, acetylene, methanethiol, dimethyl sulfide, hydrogen cyanide, etc. absorb strongly between 3 and 4 μm. Analysis of concentrations and isotopic composition of these gasses provides key information on geochemical processes, atmospheric photochemistry, and hydrothermal and biological activity. High power $\lambda \geq 3$ μm beams are required for medical therapy, laser surgery, infrared illumination, countermeasures, etc. Compact, efficient and low cost diode lasers are often preferred components for system realization. High power diode lasers can be used either directly or as pumps for solid state/fiber/nonlinear hosts. In many cases CW operation of diode lasers is either necessary or at least favored. Laser operation at or near RT dramatically simplifies the system design.

Composition of GaInAsSb QWs of GaSb-based diode lasers emitting above 3 μm ranges from 50 to 60% of In and from 20 to 30% of As. Mid-infrared diode lasers at wavelengths above 3 μm suffer from temperature sensitivity of both threshold current and external efficiency. Several factors contribute to undesirable temperature sensitivity of the laser parameters. Among them are free carrier absorption and Auger recombination. Besides these fundamental factors there may be heterostructure deficiencies. They can cause heterobarrier carrier leakage into the cladding, carrier accumulation in the waveguide core and thermal population of useless energy states inside and nearby the active QWs. These deficiencies can be eliminated by improvement of the material quality and by designing the laser heterostructure with strong carrier confinement.

It is easy to arrange for a conduction band offset to be above 300 meV in GaInAsSb QWs with AlGaInAsSb barriers. Thus in 300 meV deep and 10 – 15 nm wide QWs with the second subband quantized away by more than 100 meV there is only one electron subband that is populated at RT. At the same time the valence band offset can easily become inadequate in GaSb-based material system. The heavy hole subband separation is also small - about 15 meV between the two topmost subbands. Valence band states in the barriers and in the higher order

hole subbands can unfavorably increase the number of states available for population in the valence band. Thus one of the critical design tasks is to minimize the number of states in the valence band that are available for population.

The in-plane effective mass in the fundamental heavy hole subband can be reduced nearly to the level of electron effective mass by compressive strain of about 1 %. The strain values beyond that range have minor effect on the band-edge heavy-hole density of states, since at such high strain the heavy-hole and light-hole subbands are already well separated in energy. The population of the second heavy hole subband is minimized by use of relatively narrow QWs. The barrier state population should be minimized by constructing QWs with adequate hole confinement energies.

Performance of the GaSb-based type-I QW diode laser with wavelength above 2.5 μm was improved after the quinternary AlGaInAsSb alloy was introduced to replace quaternary AlGaAsSb as a barrier material. An increase of the As composition in any of Sb-based alloys tends to lower the position of the valence band on the absolute energy scale. Thus strong hole confinement requirement can be realized by minimizing As composition in GaInAsSb QW and maximizing As composition in AlGaInAsSb barrier materials. This can be realized by maximizing compressive strain in quaternary QW and by maximizing In and Al compositions in quinternary barrier materials. Compressively strained QWs require less As and benefit from heavy-light hole splitting. Quinternary AlGaInAsSb alloys with increased In and Al compositions require more As to maintain lattice matching to GaSb substrate.

Figure 1 illustrates the benefits of using quinternary AlGaInAsSb barriers in 3.1 μm lasers. Replacement of the quaternary $Al_{0.35}Ga_{0.65}As_{0.03}Sb_{0.97}$ with quinternary $Al_{0.2}Ga_{0.55}In_{0.25}As_{0.24}Sb_{0.76}$ barrier alloy improves the hole confinement by about 100 meV (Figure 1a) and leads to twofold decrease of RT threshold current density (Figure 1b). Again, at low temperatures the difference tends to disappear since hole confinement offered by both types of barriers becomes equally adequate.

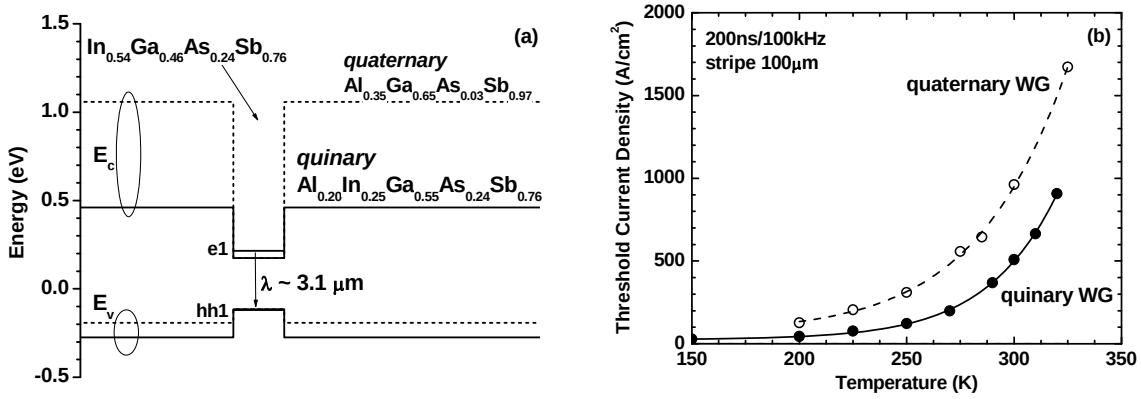

Figure 1. (a) Calculated band alignment for 3.1 μm emitting lasers. Solid line shows the band edges for QW materials and for quinternary AlInGaAsSb barriers. The dashed line shows the band edge position for quaternary AlGaAsSb alloys. (b) Temperature dependences of the threshold current density for 3.1 μm emitting lasers with AlGaAsSb quaternary and AlGaInAsSb quinternary barriers.

It should be noted that neither detailed studies of the optical properties nor detailed development of the growth procedure of the quinternary AlGaInAsSb material was performed yet. Carrier transport issues were identified in the course of optimization of the laser waveguide heterostructure with aforementioned quinternary alloy as a waveguide core. Three laser

heterostructures were grown with $Al_{0.2}Ga_{0.55}In_{0.25}As_{0.24}Sb_{0.76}$ waveguide core widths of 470 nm, 1070 nm and 1470 nm. The lasers emit near 3 μm at RT. Laser heterostructure parameters other than the waveguide core widths were nominally kept the same for all three lasers. Figure 2a shows pulsed (200 ns, 10 kHz) light-current characteristics measured at RT for 1-mm-long uncoated devices.

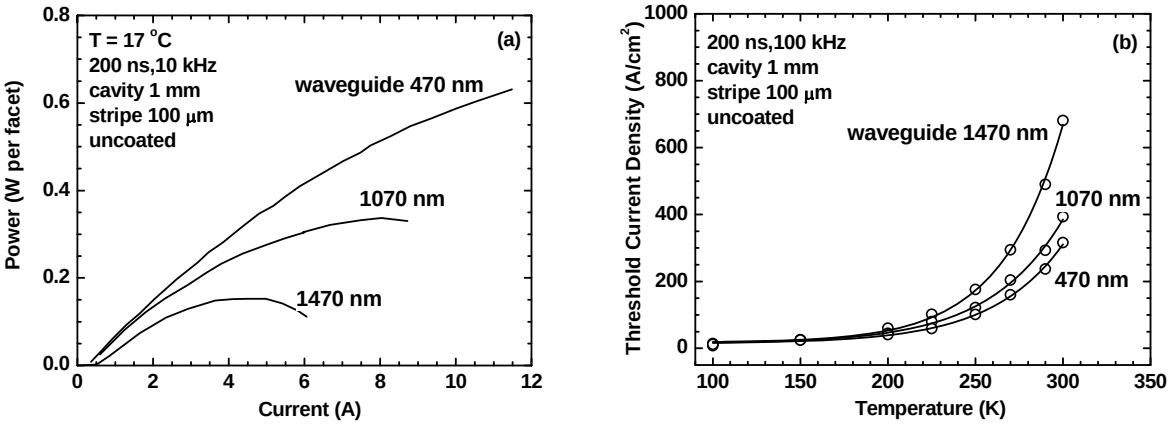

Figure 2. (a) Pulsed (200 ns, 10 kHz) light-current characteristics and (b) Temperature dependence of the threshold current density for 1-mm-long, 100-μm-wide, uncoated 3 μm lasers having different waveguide widths.

The light-current characteristics demonstrate the roll-over for all three structures that becomes more severe with increasing the waveguide width. Figure 2b shows the threshold current densities measured in wide temperature range for three structures. At 150 K all three devices have very low threshold current density of about 25 A/cm^2 that gets increased with temperature at the rates dependent on waveguide width. At 300 K the threshold current density is more than two times higher for devices with the widest waveguide than for lasers with the narrowest one.

Roll-over of the light-current characteristics in devices with broadened waveguide can be accounted for by the carrier transport constraints in waveguide region. Accumulation of the free carriers in waveguide regions between claddings and two-QW active can lead to reduction of the slope efficiency due to both free carrier absorption and recombination.

Analysis of the dependence of the threshold current density on waveguide width should take into account the distribution of the optical field in laser heterostructure. Change of optical field distribution leads to 1.7 times higher optical confinement factor in lasers with 470-nm-wide waveguides than in devices with 1470-nm-wide ones. Enhancement of the optical confinement factor should improve the differential gain in narrow waveguide lasers.

Figure 3a shows the experimental dependences of the peak modal gain on current measured by Hakki-Paoli method for all lasers. The differential gain of the devices with the narrowest waveguide is about 2.5 times higher than in lasers with the widest waveguide, i.e. the experimental rate of the differential gain increase exceeds the growth of the optical confinement factor. The enhancement of the differential gain is facilitated by improved device injection efficiency (Figure 3b). Since the diffusion current through narrowed waveguide can be supported by lower carrier concentration it is expected that the waveguide recombination current is smaller in devices with 470-nm-wide waveguide then in lasers with 1070 and 1470-nm-wide waveguides. Figure 3b shows that the broadening of the waveguide promoted the reduction of the internal loss as expected. However, the combined effects of the carrier transport through

waveguide and reduction of the MQW optical confinement factor did not allow the 3 μm lasers to benefit from associated internal optical loss reduction. This indicates possibility of further device performance enhancement after detailed material development studies are completed and carrier mobility in quinternary material might get improved.

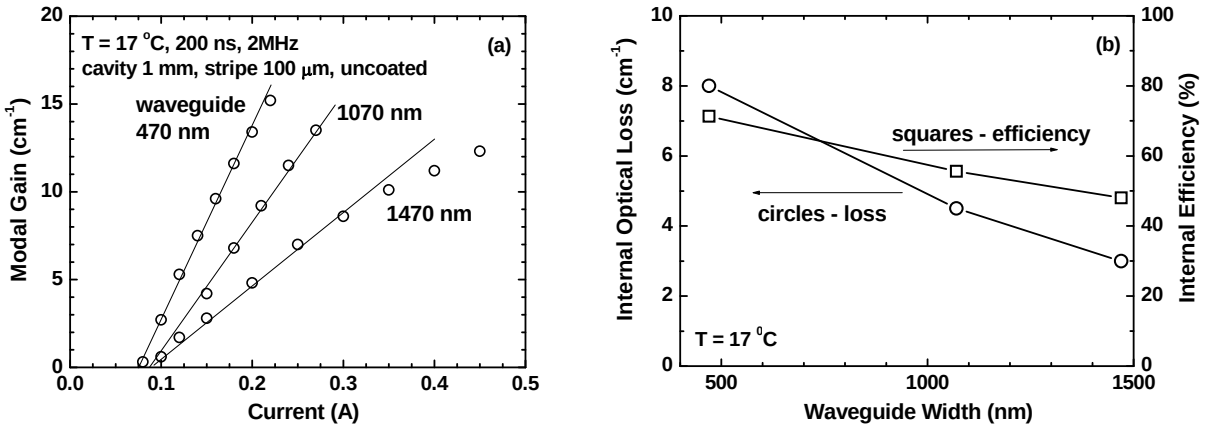

Figure 3. (a) Current dependences of the peak modal gain for 3 μm lasers with different waveguide widths, and (b) Dependence of the internal optical loss and internal efficiency on waveguide width.

Laser heterostructures with heavily compressively strained QWs with quinternary barriers were developed to produce diode lasers operating at RT in continuous wave regime in spectral region from 3 to 3.4 μm. The heterostructures were grown by solid-source molecular beam epitaxy on tellurium doped GaSb substrates. The claddings were $Al_{0.85}Ga_{0.15}As_{0.07}Sb_{0.93}$ doped with tellurium and beryllium for n- (2.5 μm thick) and p-cladding (1.5 μm thick), respectively. Doping level of the part of the p-cladding layer adjacent to waveguide was kept around 10^{17} cm^{-3} to reduce internal losses associated with free hole absorption. Wafers were processed into 100-μm-wide index-guided ridge lasers by wet etching of the top-cladding layer outside of the current stripe. The values of the empirical parameters T_0 and T_1 that characterize the exponential dependences of the laser threshold current and slope efficiency on temperature were measured in pulsed regime near 300K for 1-mm-long uncoated lasers. For CW characterization the coated lasers were indium-soldered epi-side down.

Figure 4a shows the CW RT light-current and power conversion characteristics of 3 μm emitting lasers. The laser active region comprised two 11-nm-wide 50-nm-spaced GaInAsSb QW with nominal indium composition of 50% and compressive strain of 1.7%. The barrier and waveguide material was $Al_{0.20}Ga_{0.55}In_{0.25}As_{0.24}Sb_{0.76}$ quinternary. Total width of the waveguide region (from n-cladding to p-cladding) including double-QW active was about 570nm. Laser mirrors were cleaved and coated for mirror reflectivity of below 5% for anti-reflection (AR) and above 90% for high reflection (HR). The maximum power of 360 mW was achieved at the current of 4.6 A at coolant (water) temperature of 17°C. The power conversion efficiency was better than 4% for the whole range of operation with maximum value approaching 9% at output power level of about 120 mW. The CW threshold current density was 200 A/cm^2 (100 A/cm^2 per QW). The voltage drop across laser heterostructure was below 1.4 V at the maximum output power level. Parameters T_0 and T_1 are 50K and 200K, respectively. The current dependence of the modal gain spectra is shown in Figure 4b. The internal optical loss of 4 - 5 cm^{-1} were estimated from Longwavelength part of the gain spectrum assuming mirror loss of about 12 cm^{-1}. The transparency current density is below 100 A/cm^2.

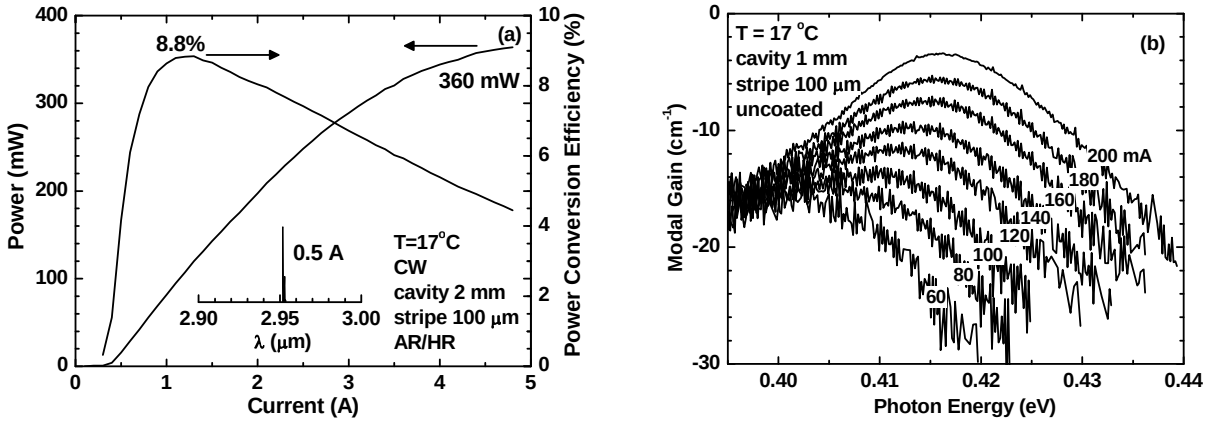

Figure 4. (a) Light-current characteristics measured in CW regime at 17°C for 2-mm-long, 100-μm-wide, AR/HR coated diode lasers with optimized design and emitting near 3 μm; (b) Current dependence of the modal gain spectra for corresponding 1-mm-long, 100-μm-wide, uncoated lasers measured in pulsed regime (200ns/2MHz).

Figure 5a shows the CW RT light-current and power conversion characteristics of 3.1 μm emitting lasers. The laser active region comprised three 13-nm-wide 1.6 % compressively strained InGaAsSb QWs separated by 50 nm wide barriers. Quinternary $Al_{0.20}Ga_{0.55}In_{0.25}As_{0.24}Sb_{0.76}$ was used in barriers and waveguide. The nominal indium composition of QWs was more than 50%. The total undoped waveguide core width was about 650 nm from p-cladding to n-cladding.

The maximum CW output power of 190 mW was achieved at the current of 3.8 A at the coolant (water) temperature of 17°C. The power conversion efficiency was better than 2% for the whole range of operation with maximum value of more than 4% at output power level of about 100 mW. The CW threshold current density was 350 A/cm^2 (about 120 A/cm^2 per QW). The internal loss is estimated to be about 8 cm^{-1} (Figure 5b). The values of the parameters T_0 and T_1 are 34K and 74K, respectively.

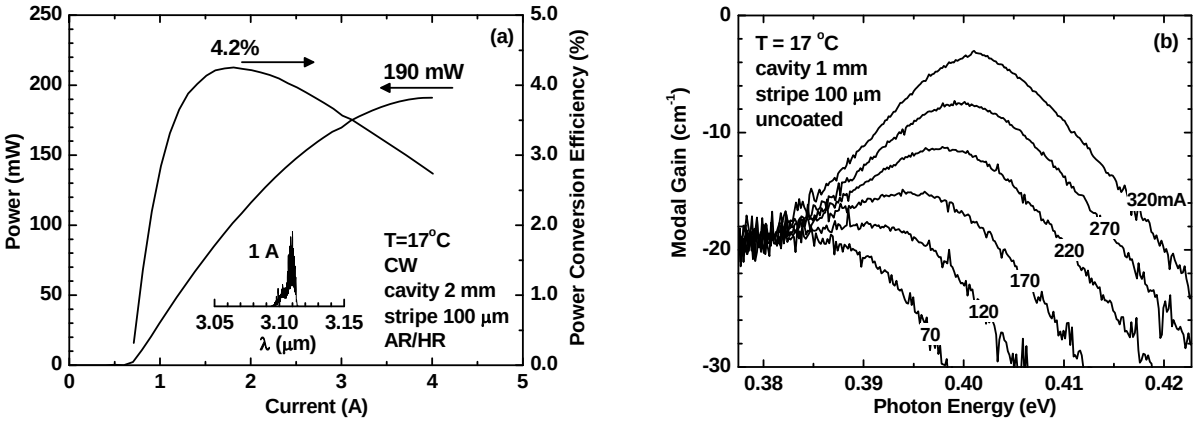

Figure 5. (a) Light-current characteristics measured in CW regime at 17°C for 2-mm-long, 100-μm-wide, AR/HR coated diode lasers emitting near 3.1 μm; (b) Current dependence of the modal gain spectra for corresponding 1-mm-long, 100-μm-wide, uncoated lasers measured in pulsed regime (200ns/2MHz).

Figure 6a shows the CW RT light-current and power conversion characteristics of 3.2 μm emitting lasers. The active layer consists of three 13-nm-wide InGaAsSb compressively-strained

QWs (1.6%) separated by 50 nm wide barriers. The nominal indium composition of QWs was near 55%. The total undoped waveguide core width was about 650 nm from p-cladding to n-cladding. The maximum power of 165 mW was achieved at the current of 4.2 A at the coolant (water) temperature of 17°C. The CW threshold current density was less than 400 A/cm^2 (about 130 A/cm^2 per QW). The voltage drop across laser heterostructure was below 1.5 V at the maximum output power level. The internal loss is estimated to be about 9 cm^{-1} from Figure 6b.

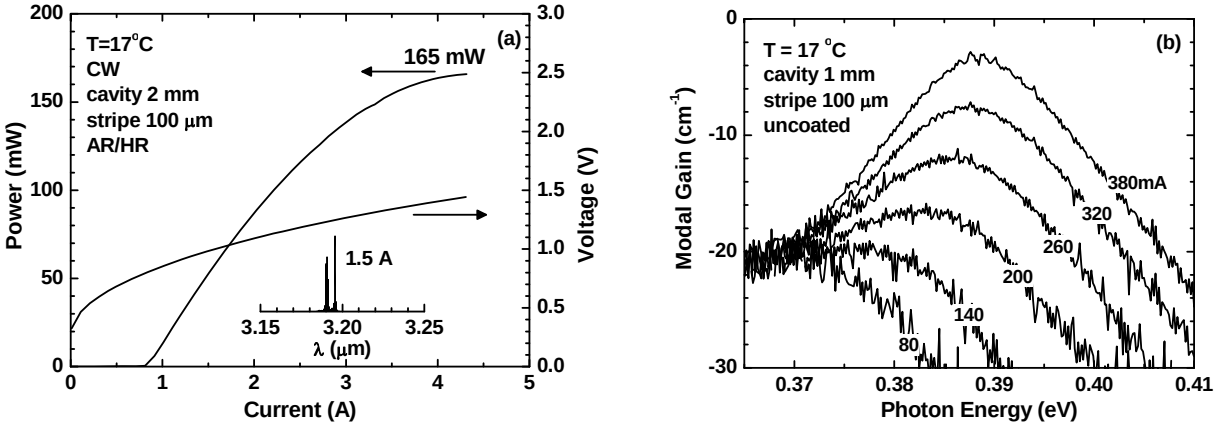

Figure 6. (a) Light-current and voltage-current characteristics measured in CW regime at 17°C for 2-mm-long, 100-μm-wide, AR/HR coated diode lasers emitting near 3.2 μm; (b) Current dependence of the modal gain spectra for corresponding 1-mm-long, 100-μm-wide, uncoated lasers measured in pulsed regime (200ns/2MHz).

Quinternary $Al_{0.22}Ga_{0.46}In_{0.32}As_{0.30}Sb_{0.70}$ was used in barriers and waveguide. The increase of indium content in the barriers from 25% to 32% increases the valence band offset between QWs and the barriers. The experiment showed that 32% of indium in AlGaInAsSb barrier improves the characteristics of 3.2 μm emitting lasers. Figure 7 plots the current dependences of the peak modal gain measured for 3.1 μm emitting laser heterostructures (Figure 5) as well as 32 μm emitting lasers heterostructures having different barrier composition, namely, the same as in 3.1 μm emitters and with increases In and As contents. Clearly, increased In and As composition led to improved differential gain and decreased threshold current densities.

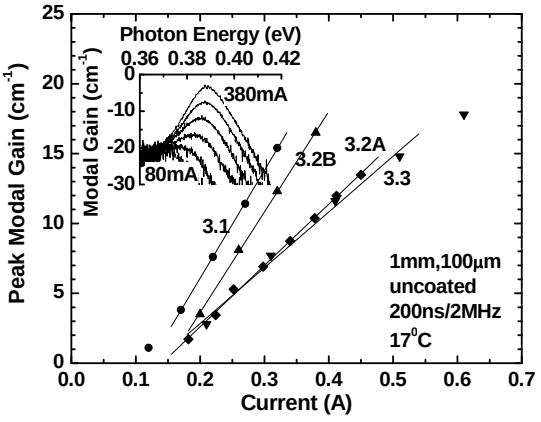

Figure 7. Dependences of the peak modal gain on current of four 1-mm-long, 100-μm-wide, uncoated lasers emitting in spectral region from 3.1 to 3.3 μm at 17 °C. Inset shows original gain spectra of laser emitting at 3.2 μm (laser B) for injection currents varying from 80 mA to 380 mA in increments of 60 mA.

Diode lasers emitting in spectral region from 3.1 to 3.3 μm and with adequate hole confinement operated in CW up to above 40^0C (Figure 8).

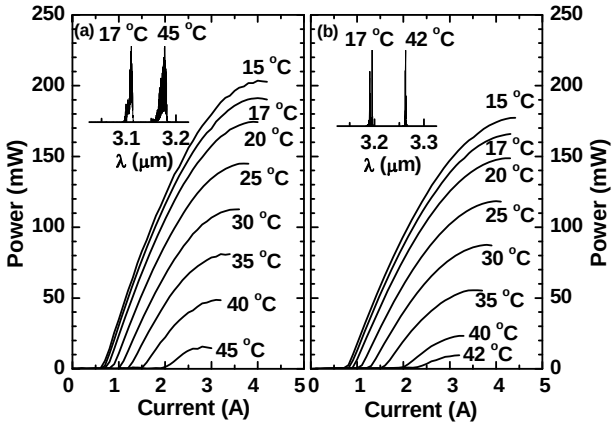

Figure 8. CW output power and spectral characteristics measured above room temperature for mm-long, AR/HR coated, 100 μm wide lasers emitting at (a) 3.1 μm and (b) 3.2 μm.

Figure 9a shows the CW RT light-current and power conversion characteristics of 3.4 μm emitting lasers. The active region consisted of three 13-nm-wide 1.5 % compressively-strained $In_{0.57}Ga_{0.43}As_{0.29}Sb_{0.71}$ QWs separated by 50-nm-wide $Al_{0.22}In_{0.32}Ga_{0.46}As_{0.30}Sb_{0.70}$ barrier layers. Waveguide core was formed by the barrier alloy of 250 nm wide on both sides of active region. More than 40 mW of CW output power was obtained at 12 °C. Increase of the heatsink temperature to 27 °C led to twofold increase of the threshold current. Voltage drop across laser heterostructure was below 1.5 V at the maximum output power level. More than 5 mW of CW output power was available at 27 °C with wavelength near 3.44 μm. The internal loss is estimated to be about 9 cm^{-1} (Figure 9b).

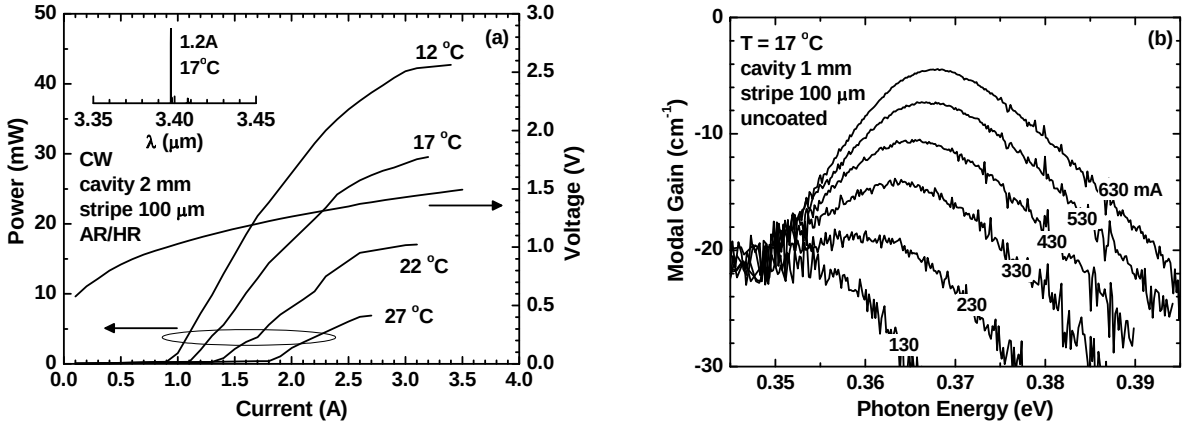

Figure 9. (a) Temperature dependence of light-current characteristics and voltage-current characteristics (17°C) measured in CW regime for 2-mm-long, 100-μm-wide, AR/HR coated diode lasers emitting near 3.4 μm; (b) Current dependence of the modal gain spectra for corresponding 1-mm-long, 100-μm-wide, uncoated lasers measured in pulsed regime (200ns/2MHz).

Increase of the laser wavelength from 3 to 3.4 μm was accompanied by threefold increase of the threshold current density and corresponding reduction of the device efficiency. It is hardly feasible that probability of individual Auger recombination events could increase threefold when

bandgap is reduced by only about 10 %. However, to reduce the active region bandgap by 10 % the GaInAsSb QWs of 3.4 μm lasers were made wider and incorporated more Indium than QWs of 3 μm lasers. Extra Indium requires extra Arsenic to maintain pseudomorphic growth. Increased As concentration moves QW valence band edge down on the absolute energy scale thus degrading the hole confinement. Figure 10 illustrates this trend by plotting the compositional dependence of the band edge positions of the GaInAsSb alloy with 1.5 % compressive strain.

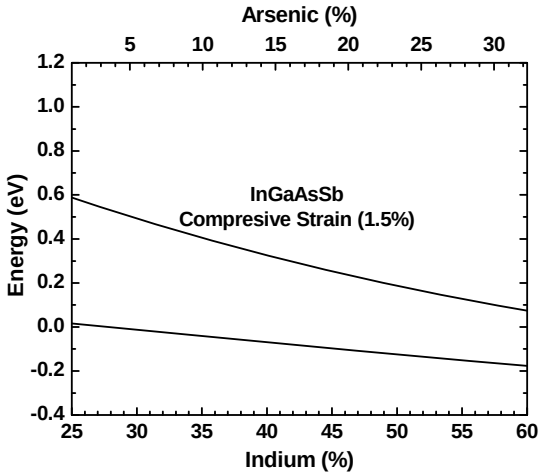

Figure 10. Calculated positions of the band edges on absolute energy scale for GaInAsSb QW alloy with 1.5 % of compressive strain with respect to GaSb substrate.

Increase of QW Indium contents from about 25% (2.2 μm RT emission wavelength in 10 - 15 nm wide QWs) to about 60% (3.5 - 4 μm RT emission wavelength) lowers the QW valence band edge by about 200 meV. Unless barrier material is correspondingly adjusted, the hole confinement will degrade and can even completely disappear. Poor hole confinement increases the number of states in valence band available for thermal population thus increasing threshold carrier concentration and triggering the Auger and other temperature-activated processes that are detrimental to high power RT operation of diode lasers. Design approach based on metamorphic growth of Sb-based diode laser heterostructures can address the issue of lack of hole confinement. The details will be described in the next section.

(b) Metamorphic antimonide diode lasers.

The poor hole confinement of In-rich GaInAsSb alloys can be partly recovered if QW is grown on substrates with lattice constant bigger than that of GaSb. Figure 11a illustrates this concept by plotting the band edges for 1.5% strained QW containing 60% Indium. Calculations predict the increase of the absolute position of the valence band edge in about 100 and 200 meV when the reference lattice constant is increased, correspondingly, by 1% and 2% from that of GaSb. Figure 11b plots band edges of the quinary AlGaInAsSb barrier material lattice matched to this new lattice. Increase of the lattice constant of AlGaInAsSb quinary alloy can be achieved by replacing Ga with In while keeping the As composition unchanged. Thus if the reference lattice constant is increased from that of GaSb, the QW As composition can be reduced while that of the barrier remains unchanged.

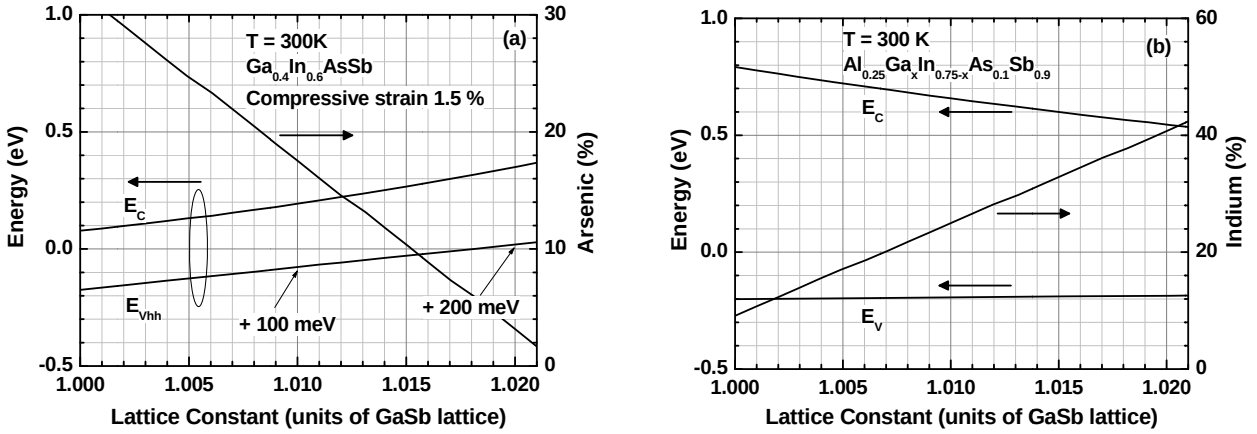

Figure 11. Calculated positions of the band edges on absolute energy scale for: (a) $Ga_{0.4}In_{0.6}As_ySb_{1-y}$ QW alloy with y adjusted to have 1.5 % of strain on the virtual substrate; (b) $Al_{0.25}Ga_xIn_{0.75-x}As_{0.1}Sb_{0.9}$ barrier alloy with x adjusted to lattice match to the virtual substrate.

The availability of high-quality virtual substrates with lattice constant larger than that of GaSb would allow development of mid-infrared laser heterostructures with improved carrier confinement in the active region which would allow extended operating wavelength and enhanced output power levels for the GaSb-based type-I QW diode lasers. One of the possible ways to increase the reference lattice constant from that of GaSb is to use GaInSb or AlGaInSb alloys as a substrate [1]. At present moment the corresponding bulk substrates are not available. Metamorphic molecular beam epitaxy can be used to grow GaInSb or AlGaInSb virtual substrates with designed lattice constant on top of GaSb substrates. The lattice constant can be adjusted by varying In content. Graded buffers can be used to accommodate lattice mismatch between parent and virtual substrates and confine corresponding misfit dislocation network [2].

Linearly graded GaInSb buffers were developed and $Ga_{0.87}In_{0.13}Sb$ virtual substrates with lattice constants ~0.8 bigger than that of GaSb were realized. The virtual substrates were grown on top of 2-μm-thick GaInSb buffer layers. The buffer layers had a linearly graded native lattice constants. Figure 12a shows the (004) θ/2-θ scan measured for the epi structure containing 500 nm thick $Ga_{0.87}In_{0.13}Sb$ virtual substrate with lattice constant 0.8% larger than that of GaSb.

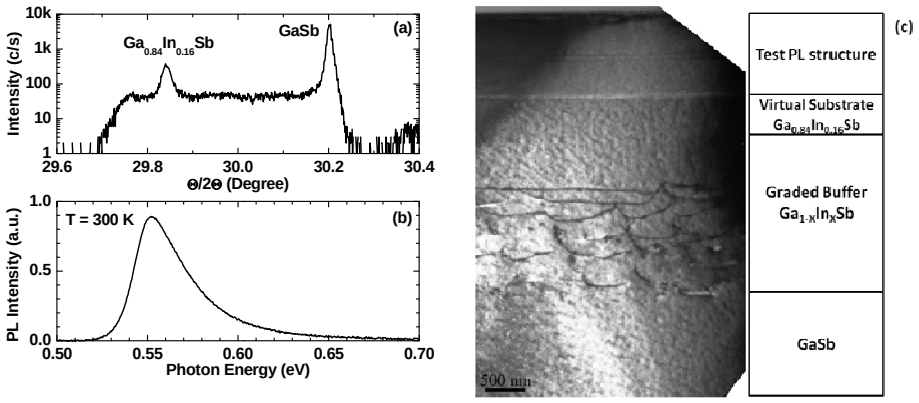

Figure 12. (a) High resolution x-ray diffraction (HRXRD) (004) θ/2-θ scan of an unstrained $Ga_{0.84}In_{0.16}Sb$ virtual substrate grown on a GaInSb graded buffer layer; (b) Room-temperature PL spectrum of the test structure grown on the virtual substrate; (c) XTEM of the test structure grown on the virtual substrate.

The rightmost intensive peak corresponds to GaSb substrate. The flat shoulder to the left of the substrate peak corresponds to the graded buffer. The reflex from $Ga_{0.87}In_{0.13}Sb$ virtual substrate layer is clearly seen. Intensive photoluminescence was observed at RT from the test structure grown directly on top of the virtual substrate (Figure 12b). The test structure consisted of two 10 nm wide compressively strained $Ga_{0.65}In_{0.35}Sb$ QWs separated by 50 nm of $Al_{0.25}Ga_{0.64}In_{0.11}Sb$ alloy. Figure 12c shows a cross sectional transmission electron microscopy micrograph of the test structure grown on the virtual substrate. The misfit dislocation network is fully confined in the bottom 1500 nm of the graded buffer layer.

Virtual substrate with 0.8 % bigger lattice constant than that of GaSb was used to demonstrate the compatibility of the metamorphic growth with high power diode laser technology, namely high power 2.2 μm lasers. The laser heterostructures designed for operation at a wavelength of 2.2 μm were grown on the $Ga_{0.87}In_{0.13}Sb$ virtual substrate. The laser active region and the waveguide core resembled the test structure described above. The n- and p-cladding layers were Te- and Be-doped $Al_{0.85}Ga_{0.07}In_{0.08}Sb$. The graded bandgap, heavily doped transition layers were introduced between the substrate and the n-cladding and between the p-cladding and the p-$Ga_{0.87}In_{0.13}Sb$ cap layers. Figure 13 plots the power and power conversion characteristics measured for diode lasers with cavity lengths of 2 and 3 mm.

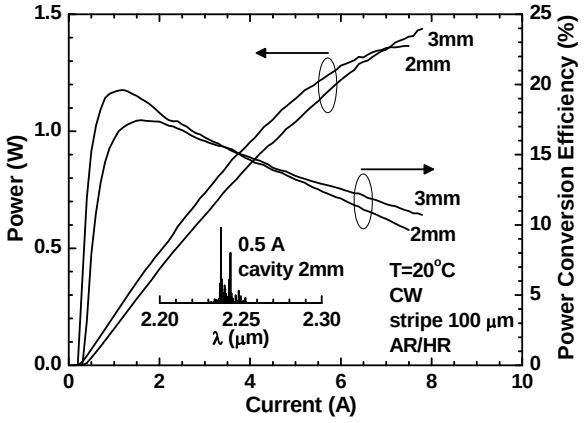

Figure 13. CW power and power conversion characteristics of 100-μm-wide 2- and 3-mm-long AR/HR coated metamorphic devices measured at 20 ^{0}C. Inset shows the laser spectrum at 5 A.

The devices demonstrate a CW threshold current density of below 150 A/cm^2 at 20 °C. The maximum CW output power above 1.4 W was obtained from the 3-mm-long lasers at 20 °C. The power conversion efficiency peaked at about 20% and remained above 10% at the maximum output power level. Parameters $T_0 \approx 70$ K and $T_1 \approx 230$ K were measured in the temperature range from 20 to 70 °C for 1-mm-long uncoated lasers in pulsed regime. The voltage drop across the laser heterostructure remained below 2 V at the maximum output power level. It should be noted that devices were processed following a standard double-side contact diode laser technology in which current flows through the virtual substrate and the graded buffer layer. Relatively low voltage drops measured across the metamorphic laser heterostructures indicate that the strain relaxed section of the graded GaInSb buffer does not obstruct the current flow. The experimental results demonstrate the compatibility of the proposed metamorphic laser heterostructure growth technology with the high power diode laser technology. We are actively working on development of the metamorphic laser heterostructures emitting in spectral region from 3 to 4 μm and demonstrating improved carrier confinement.

(c) Single spatial mode 3 – 3.2 μm diode lasers.

The devices were developed in collaboration with Jet Propulsion Laboratory

Many important gases and other chemical agents can be remotely detected by tunable laser spectroscopy in spectral region near and above 3 μm. For instance, methane, ethane, acetylene, methanethiol, dimethyl sulfide, hydrogen cyanide, etc. absorb strongly between 3 and 4 μm. Analysis of concentrations and isotopic composition of these gasses provides key information on geochemical processes, atmospheric photochemistry, and hydrothermal and biological activity.

We developed shallow etched, narrow ridge Fabry–Perot 3.0 – 3.2 μm semiconductor diode lasers operating in CW regime up to 333 K. By comparing lasers with and without thick dielectric coating, we show that the optical loss in narrow ridge devices can be significantly reduced by thick dielectric coating and the current spreading does not impede laser operation. Realization of these devices is an important step in the development of single frequency distributed feedback (DFB) mid-IR diode lasers for spectroscopic applications.

Narrow ridge waveguide lasers were fabricated using an inductively coupled plasma (ICP) reactive ion etching that was optimized to achieve vertical ridge sidewalls with excellent surface smoothness (Figure 14). After waveguide definition, thin (300 nm) or thick (800 nm) layers of silicon nitride were deposited. The SiN dielectric layer serves as an insulation layer for the top metal contact and reduces an overlap of the optical mode with the metal layer, thus lowering optical loss. Next, a narrow window was opened in silicon nitride on top of the laser ridge that was followed by evaporation of Ti/Pt/Au metal contact and deposition of a thick gold layer to improve heat dissipation. The laser wafer was thinned to approximately 100 μm and bottom Ti/Pt/Au metal contact was evaporated. Finally, the wafers were cleaved into bars with facets left uncoated and lasers were mounted junction side-up on copper mounts with In solder.

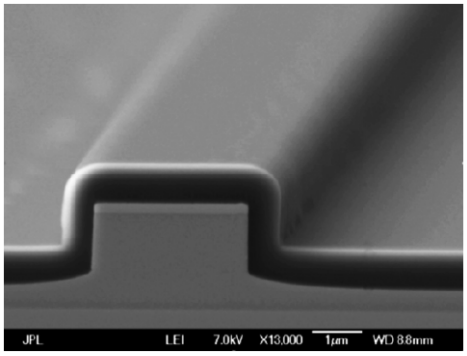

Figure 14. Scanning electron microscope (SEM) image of the cleaved mirror of the ridge waveguide covered by thick (800 nm) layer of silicon nitride.

Figure 15a shows the CW light–current–voltage (LIV) characteristics of 2 mm long 13 μm wide ridge waveguide devices with thin Si_3N_4 coating. These lasers operate in CW regime up to 313 K and the emission wavelength is 3.0 μm at the 310 K temperature (Figure 15a, inset). CW LIV characteristics of 2.5 mm long 5 μm wide ridge waveguide devices with thick Si_3N_4 coating are shown in Figure 15b. The maximal operating temperature of these devices is much higher—up to 333 K—and their output power reaches 5 mW at ambient temperature. The laser emission wavelength is 3.1 μm at 280 K (Figure 15b, inset); it increases to 3.2 μm at the maximum operating temperature of 333 K (not shown). The laser bias is approximately 1 V, so these devices require less than 0.2 W of electrical power for ambient temperature operation with power levels of approximately 1 mW which are sufficient for many spectroscopic applications.

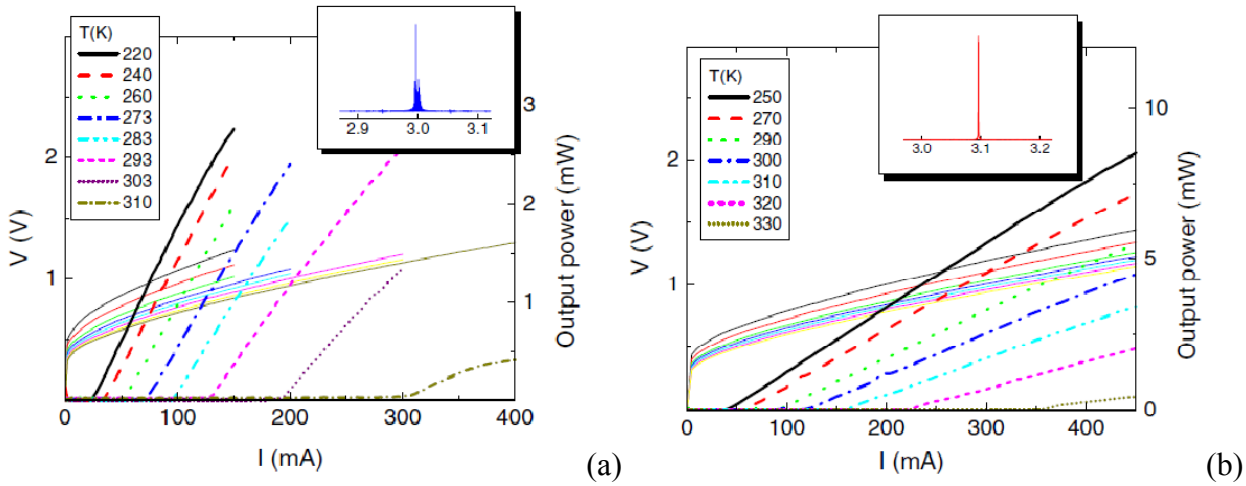

Figure 15. (a) CW light–current–voltage characteristics of 2 mm long 13 μm wide ridge waveguide devices with thin Si_3N_4 coating at various temperatures as indicated on the graph. Insert: the laser emission spectrum at T = 310 K.; (b) CW light–current–voltage characteristics of 2.5 mm long 5 μm wide ridge waveguide devices with thick Si_3N_4 coating operating at various temperatures as indicated at the graph. Insert: the laser emission spectrum at 290 K.

The advantage of thick Si3N4 for narrow ridge devices is clearly noticeable when laser threshold current density versus temperature is examined for different ridge widths (Figure 16). In samples with thin dielectric (sample A), the difference in the threshold current densities between 7 and 13 μm wide ridge lasers is large for all measured temperatures above 220 K and the maximum operating temperature of 7 μm wide ridge lasers is 260 K which is 50 K lower than 310 K measured for 13 μm ridge lasers. In contrast, in samples with thick dielectric (sample C) the differences in the threshold current densities between lasers with ridge widths varying from 5 to 9 μm are small, so all of them have maximal operational temperature above 333 K. Moreover, the device with a 5 μm wide ridge, which is narrow enough to provide sufficient overlap between the optical mode and the grating in the laterally coupled DFB, can operate above room temperature.

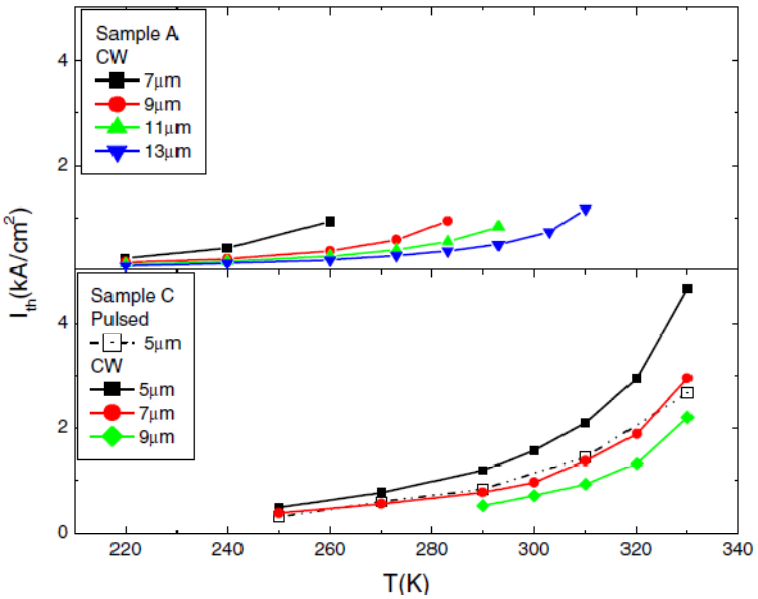

Figure 16. Threshold current density versus temperature for lasers with thin (sample A) and thick (sample C) dielectric coatings and with different ridge widths as indicated on the graph.

Thick dielectric coating can increase the device's thermal resistance thus impeding laser performance. However, the thermal loading effect is not strong in the current devices as can be inferred from comparing pulsed and CW threshold current densities for 5 μm devices (Figure 16, bottom). For threshold current densities 2 kA/cm^2, the laser's operating temperature is 308 K in CW mode and 321 K in pulsed mode that gives a temperature increase of the active region due to self-heating effects of about 13 K. This relatively small value of thermal loading effect can be attributed to several factors: (1) lower power consumption of the devices, (2) good thermal conductivity of Si_3N_4, and (3) presence of thick electroplated gold coating. The thermal resistivity calculated from temperature difference and from the laser power consumption is about 65 K/W for 2.5 mm long 5 μm wide ridge waveguide lasers with thick Si_3N_4 coating.

The modal gain spectra and total optical loss were measured, using the Hakki–Paoli technique, from the optical spectra of the lasers operating below threshold at ambient temperature. Internal optical loss was estimated by subtracting the calculated mirror loss assuming 30% reflectivity from uncoated cleaved mirrors. In samples with thin dielectric the mode interaction with the sidewall metal starts to contribute significantly to the total internal optical loss at ridge widths narrower than 20 μm; hence, the loss of 10 μm ridge is four times larger than that of the broad area devices (100 μm ridge width). In the devices with thick dielectric, the optical loss from the side wall metal starts to contribute only for ridges narrower than 10 μm, yet 3–5 μm ridge devices have internal optical losses only twice that of the broad area devices. These results indicate that the optical loss rather than the current spreading (which does not depend on the dielectric thickness and increases for the narrow ridge devices) is the main factor responsible for decreasing performance of the narrow ridge devices with thin Si_3N_4 coating. Interaction of the optical mode with the metal on the top and on the sides of waveguide ridge as well as with surface plasmons existing on semiconductor/metal interface results in the optical waveguide loss. This loss is proportional to an overlap of the optical mode with the metal and so it is essential to reduce the overlap to achieve good laser performance. This can be realized by increasing the ridge waveguide width and by using thick dielectric coating, where the latter method is essential for development of DFB lasers.

(d) Mid-infrared light emitting diodes.

High brightness and high efficiency broadband light sources for the spectral range 2 – 5 μm are in high demand for industrial chemical sensing, process monitoring and mid-infrared imaging. A central element of these technologies is an efficient mid-infrared LED capable of quasi-CW RT operation. The type-I QW active region developed for diode lasers can be used as an active region of mid-infrared LEDs. It should be noted that active region based on interband transition is equally useful for both laser and LED development while inter subband quantum cascade active regions demonstrate extremely low radiative efficiency without stimulated emission. A combination of quinternary AlGaInAsSb barriers and quaternary compressively strained GaInAsSb QWs in the device active area allowed for improvement in hole confinement and balancing of the density of states in conduction and valence bands.

Figure 17 shows schematically the two types of LEDs that were studied, with deep etched mesa and not etched. The first type was used for material parameters characterization and the second type was later utilized for LED individually addressable array development. The contrast between the pixels and the background is much better in the case of deep etched mesas. In the array with no etched grooves, the current spreading leads to emission from the area between the pixels.

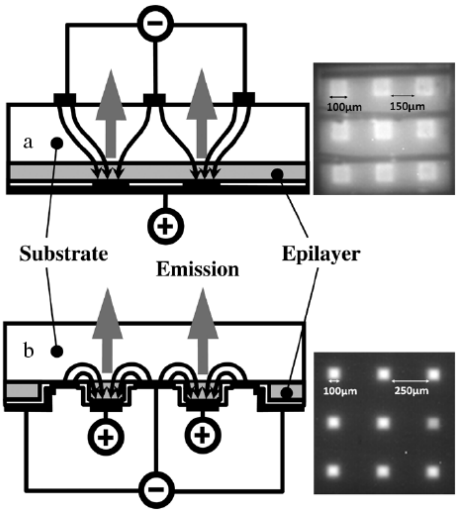

Figure 17. Schemes and mid-IR images of (a) non- addressable and (b) addressable LED arrays.

The emission spectra were measured with a Fourier transform infrared (IR) spectrometer and InSb photodetector. The emission spectrum of the device is presented in Figure 18a. Increasing the In content in the QW and adjusting As content to keep the strain at 1.5% made it possible to push the peak operation wavelength to 3.66 μm. As the temperature changed from 300 to 100 K, the emission quantum energy increased at the rate of 0.25 meV K. The fringe structure is due to interference in the device substrate. The additional spectral peak at the high-energy side of the spectrum is probably due to optical transition from the higher electron sub-band.

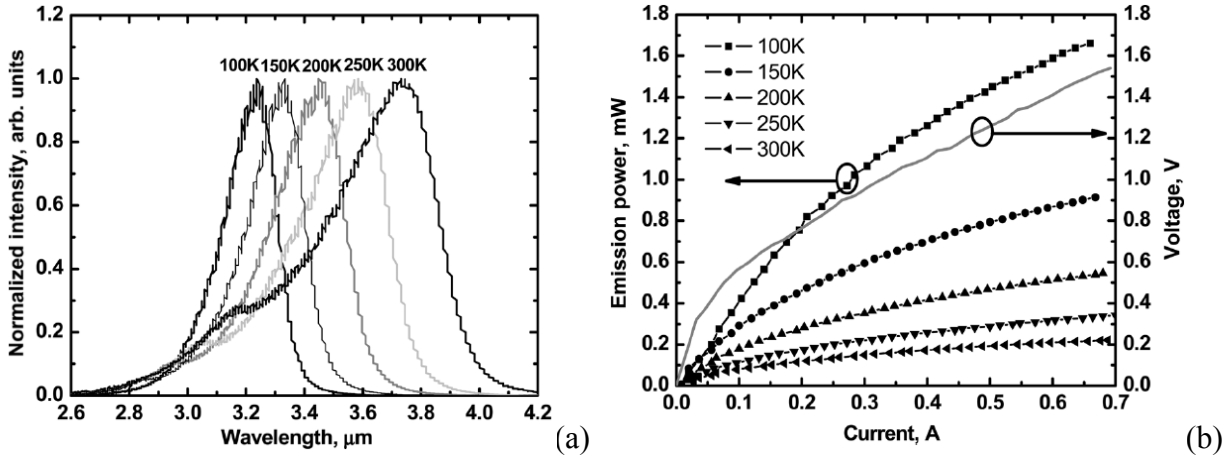

Figure 18. (a) LED spectra at different temperatures; (b) Dependences of the output power versus bias current for non-addressable 3x3 LED array at different temperature and the current–voltage dependence at room temperature.

The output power of the device was measured using an InSb photodiode and a lock-in amplifier. A gold plated integration sphere with a large aperture was used for light collection and homogenizing the radiation. Using an integration sphere with a large input aperture made the measured output power much less sensitive to the optical adjustment accuracy. This allowed direct, reliable, and reproducible measurements of the total output power of the emitter. The total output power of the 3x3 array (total emitting area 300 x 300 μm^2) with no etched grooves is shown in Figure 18b. The output power increased at low temperatures and reached 1.6 mW at 0.6 A (100 K).

We performed comparison of the LEDs developed at Stony Brook University with those available commercially. Figure 19 plots the RT output power versus current for 3.65 μm emitters made at Stony Brook and samples acquired from Boston Electronics. Our devices demonstrate higher output power at 20^0C despite no immersion lens or any other outcoupling element was utilized unlike in Boston Electronic devices using specially designed components for enhanced outcoupling.

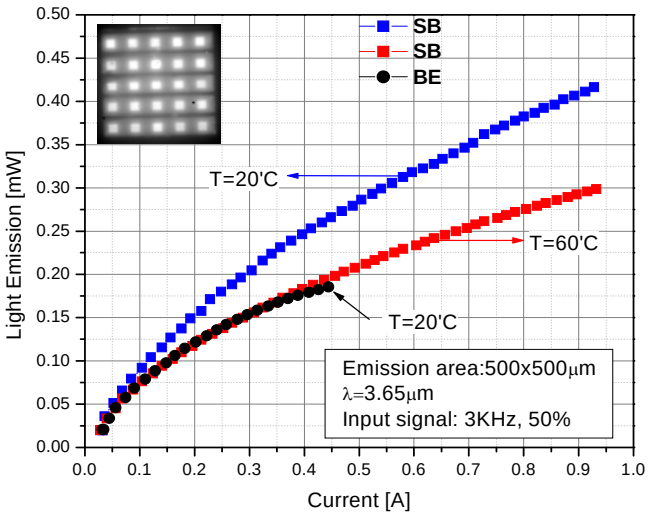

Figure 19. Comparison of Stony Brook's 3.65 μm emitting LEDs (squares) with those acquired from Boston Electronics (circles). Emitting area in both cases was 500 by 500 μm^2. The inset shows the infrared image of Stony Brook's LED.

Development of the bulk GaInAsSb active region allowed the RT operation of the LEDs with wavelength above 4 μm (Figure 20).

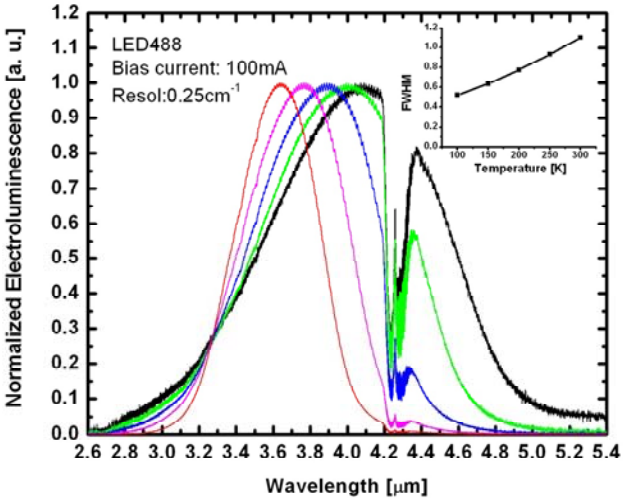

Figure 20. Temperature dependence of the output spectra of the LEDs with bulk active region.

A dual wavelength LED with separate control over the "color" intensities can make an effective emission source which combines both sensing and reference wavelengths within one device. The band diagram of the dual wavelength LED structure designed and developed at Stony Brook University is presented in Figure 21. The device comprises two LED sections

grown on the same wafer and separated by a p-doped GaSb contact layer. The color intensities are controlled separately through the application of bias voltages between the top layer and the substrate with respect to the middle contact

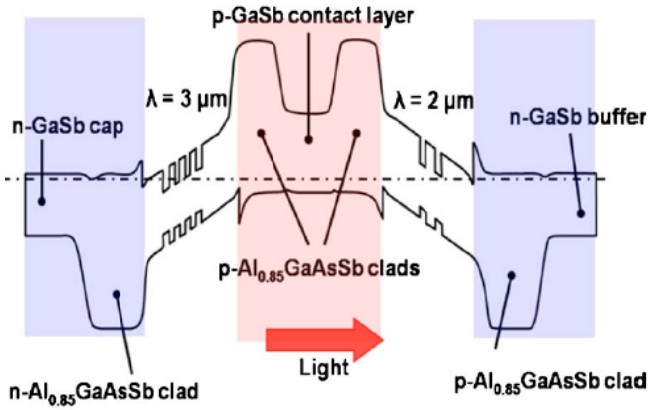

Figure 21. Schematic band diagram of the dual color LEDs.

The processed dual color LED structure and output spectra of the each LED sections are shown in Figure 22a. The electroluminescence of the dual wavelength LED was measured at room temperature (Figure 22b). The intensities of two emission peaks positioned at 2 and 3 μm can be controlled independently. The wider emission peak of the top LED λ = 3 μm may be due to higher non uniformity of the longer wavelength material. The distortion of the emission pattern near 2.7 μm is due to water absorption.

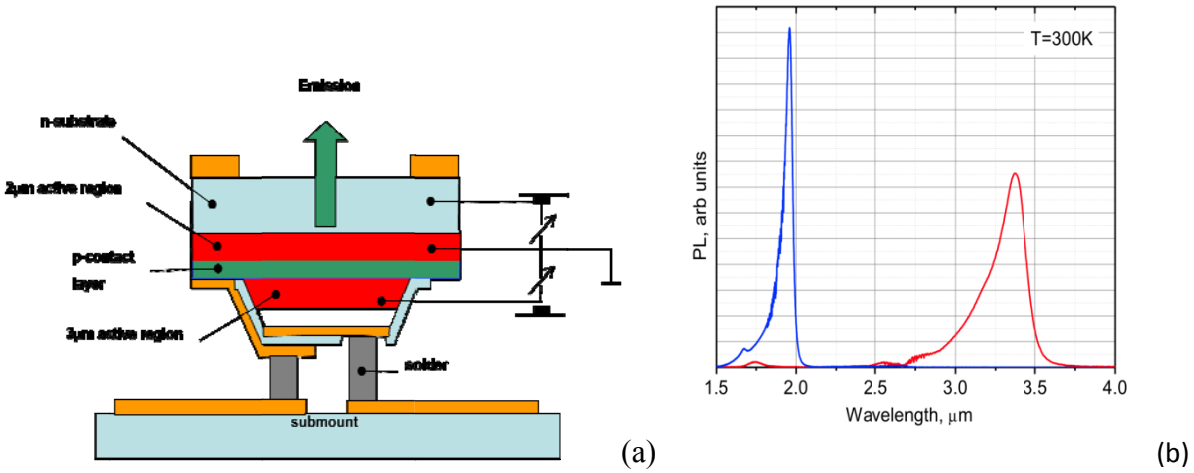

Figure 22. (a) Structure of the processed dual color LED; and (b) Spectra of the output from each of the LED sections.

The dependence of optical power of each LED versus bias current is shown in Figure 23. The bottom LED λ = 2 μm produced the optical power as high as 2.8 mW under quasi-CW (3 KHz, 50%) and 8.5 mW under pulsed (3 KHz, 1%) mode at room temperature. For the top LED λ = 3 μm, powers of 0.14 mW and 0.32 mW were obtained under quasi-CW and pulsed modes, respectively. A possible reason for saturation of the power is device heating due to limited thermal conductivity of the silicon submounts used. This effect is more pronounced for the bottom LED since a heat sink is farther away from the bottom LED λ = 2 μm than the top LED

$\lambda = 3$ μm. Hole heterobarrier leakage can also contribute to the rollover of the output power at high current injection.

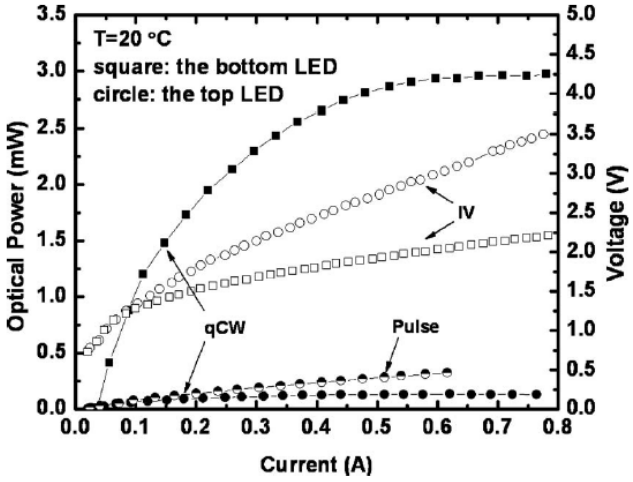

Figure 23. Light-current-voltage characteristic for the dual wavelength LED. Closed and half closed symbol for the optical power vs current under quasi-CW (3 kHz, 50%) and pulsed (3 kHz, 1%) mode operation, respectively. Open symbol for the voltage vs current.

References

1 E.A. Pease, L.R. Dawson, L.G. Vaughn, P. Rotella, and L.F. Lester, "2.5-3.5 μm optically pumped GaInSb/AlGaInSb multiple quantum well lasers grown on AlInSb metamorphic buffer layers", J. Appl. Phys. 93, 3177 (2003).

2 J. Tersoff, "Dislocation and strain relief in compositionally graded layers", Appl. Phys. Lett. 62, 693 (1993).

Supported Personnel

Dr. G. Belenky, Distinguished professor, PI/PD, general project leadership

Dr. L. Shterengas, Assistant professor, co-PI, device design and technology

Dr. D. Donetsky, Assistant professor, co-PI, material characterization

Dr. S. Suchalkin, Adjunct professor, co-PI, LED development

Dr. G. Kipshidze, Senior research scientist, MBE growth

Dr. J. Chen, Graduate student
PhD in EE, May 2011, employed by Crystal IS, Inc. (Green Island, NY 12183)

Dr. T. Hosoda, Graduate student
PhD in EE, December 2011, employed by Stony Brook University

Mr. S. Jung, Graduate student
PhD in EE, expected graduation in December 2012

Mr. D. Wang, Graduate student
PhD in EE, expected graduation in December 2012

Collaborations

- "Development of the mid-IR LED technology for infrared scene projectors", Dr. E. Golden, Air Force Research Laboratory, Eglin Air Force Base.
- "A stable mid-IR, GaSb-based diode laser source for the cryogenic target layering at the Omega Laser Facility", Dr. A.V. Okishev, Laboratory for Laser Energetic, University of Rochester
- "Development of the ridge waveguide $\lambda > 3$ μm diode lasers for spectroscopy", Dr. S. Forouhar, Jet Propulsion Lab

Dissertations

Dr. T. Hosoda, "GaSb-based type-I diode lasers operating at 3 μm and above",
Stony Brook University, Department of Electrical and Computer Engineering, December 2011.

Publications

Book Chapters

G. Belenky, L. Shterengas, M. Kisin, T. Hosoda, "GaSb-based type-I quantum well diode lasers" in "Semiconductor lasers - fundamentals and applications", Woodhead Publishing, to be published in (2012).

L. Shterengas, G. Kipshidze, T. Hosoda, G. Belenky, "GaSb-based type-I laser diodes operating at 3 μm and beyond", Advanced Research Workshop on "Future Trends in Microelectronics: From Nanophotonics to Sensors and Energy", Wiley ISBN: 978-0-470-55137-0 (2010).

Scientific Journals

1. G. Belenky, L. Shterengas, G. Kipshidze, T. Hosoda, "Type-I diode lasers for spectral region above 3 μm", IEEE J. Select. Top. Quantum Electron. 17, 1426 (2011).

2. A. Soibel, C. Frez, A. Ksendzov, S. Keo, S. Forouhar, G. Tsvid, G. Kipshidze, L. Shterengas, G. Belenky, "The 3.0 – 3.2 μm wavelength range narrow ridge waveguide Sb-based semiconductor diode lasers operating up to 333 K", Semicond. Sci. Technol. 26, 095024 (2011).
3. R. Liang, J. Chen, G. Kipshidze, D. Westerfeld, L. Shterengas, G. Belenky, "High-power 2.2-μm diode lasers with heavily strained active region", IEEE Photon. Technol. Lett. 23, 603 (2011).
4. G. Kipshidze, T. Hosoda, W.L. Sarney, L. Shterengas, G. Belenky, "High-Power 2.2-μm diode lasers with metamorphic arsenic-free heterostructures", IEEE Photon. Technol. Lett. 23, 317 (2011).
5. S. Jung, S. Suchalkin, D. Westerfeld, G. Kipshidze, E. Golden, D. Snyder, G. Belenky, "High dimensional addressable LED arrays based on type I GaInAsSb quantum wells with quinternary AlGaInAsSb barriers", Semicond Sci. Technol. 26, 085022 (2011).
6. T. Hosoda, G. Kipshidze, L. Shterengas and G. Belenky, "Diode lasers emitting near 3.44 μm in continuous-wave regime at 300K", Electron. Lett. 46, 1455 (2010).
7. J. Chen, G. Kipshidze, L. Shterengas, "High-power 2 μm diode lasers with asymmetric waveguide", IEEE J. Quantum Electron. 46, 1464 (2010).
8. J. Chen, T. Hosoda, G. Tsvid, R. Liang, D. Westerfeld, G. Kipshidze, L. Shterengas, G. Belenky, "Type-I GaSb based diode lasers operating at room temperature in 2 to 3.5 μm spectral region", SPIE Proceedings 7686 (2010).
9. J. Chen, G. Kipshidze, L. Shterengas, "Diode lasers with asymmetric waveguide and improved beam properties", Appl. Phys. Lett. 96, 241111 (2010).
10. T. Hosoda, G. Kipshidze, G. Tsvid, L. Shterengas, G. Belenky, "Type-I GaSb-based laser diodes operating in 3.1 to 3.3-μm wavelength range", IEEE Photon. Technol. Lett. 22, 718 (2010).
11. J. Chen, T. Hosoda, G. Kipshidze, L. Shterengas, G. Belenky, A. Soibel, C. Frez. S. Forouhar "Single spatial mode room temperature operated 3.15 μm diode lasers", Electron. Lett. 46, 367 (2010).
12. S. Jung, S. Suchalkin, G. Kipshidze, D. Westerfeld, E. Golden, D. Snyder, G. Belenky, "Dual wavelength GaSb based type I quantum well mid-infrared light emitting diodes", Appl. Phys. Lett. 96, 191102 (2010).
13. G. Belenky, L. Shterengas, D. Wang, G. Kipshidze, L. Vorobjev, "Continuous wave operated 3.2 μm type-I quantum-well diode lasers with the quinary waveguide layer", Semicond. Science Technol. 24, 115013 (2009).
14. A.V. Okishev, D. Westerfeld, L. Shterengas, G. Belenky, "A stable mid-IR, GaSb-based diode laser source for the cryogenic target layering at the Omega Laser Facility", Optics Express 17, 15760 (2009).
15. L. Shterengas, G. Kipshidze, T. Hosoda, J. Chen, G. Belenky, "Diode lasers emitting at 3 μm with 300 mW of continuous-wave output power", Electron, Lett. 45, 942 (2009).
16. T. Hosoda, G. Kipshidze, L. Shterengas, G. Belenky, "200 mW type-I GaSb-based laser diodes operating at 3 μm. Role of waveguide width", Appl. Phys. Lett. 94, 261104 (2009).
17. S. Jung, S. Suchalkin, G. Kipshidze, D. Westerfeld, D. Snyder, M. Johnson, G. Belenky, "GaSb-based type-I quantum-well light-emitting diode addressable array operated at wavelengths up to 3.66 μm", IEEE Photon. Technol. Lett. 21, 1087 (2009).

Conference Presentations

1. S. Forouhar, C. Frez, A. Ksendzov, Y. Qiu, K. J. Franz, A. Soibel, J. Chen, T. Hosoda, G. Kipshidze, L. Shterengas, G. Belenky, "Low power consumption lasers for next generation miniature optical spectrometers for trace gas analysis," SPIE Photonics West, January 22-27 (2011), San Francisco, CA.
2. G. Belenky, L. Shterengas, G. Kipshidze, T. Hosoda, J. Chen, "Advances in the development of type-I quantum well GaSb-based diode lasers," SPIE Photonics West, January 22-27 (2011), San Francisco, CA.
3. G. Tsvid, A. Soibel, T. Hosoda, J. Chen, G. Kipshidze, L. Shterengas, C. F. Frez, S. Forouhar, G. Belenky, "Type-I GaSb based diode single lateral mode lasers operating at room temperature in 3.1-3.2 μm spectral region," SPIE Photonics West, January 22-27 (2011), San Francisco, CA.
4. L. Shterengas, G. Kipshidze, T. Hosoda, G. Tsvid, G. Belenky, "Diode Lasers Emitting above 3 μm at Room Temperature with more than 100 mW of Continuous Wave Output Power," SPIE Photonics West, January 23-28 (2010), San Fransisco, CA.
5. T. Hosoda, J. Chen, G. Tsvid, G. Kipshidze, S. Suchalkin, L. Shterengas and G. Belenky, "Diode Lasers Operating at Room Temperature in 2-3.5 μm Spectral Region", SPIE Defense, Security and Sensing, April 5-9 (2010), Orlando, FL.
6. Soibel, C. Frez, A. Ksendzov, Y. Qiu, S. Forouhar, J. Chen, T. Hosoda, G. Kipshidze, L. Shterengas, G. Tsvid, G. Belenky, "3.0-3.5μm single spatial mode diode lasers operating at room temperature," Conference on Lasers and Electro Optics, 2010 (CLEO 2010), May 16-21 (2010), San Jose, CA.
7. G. Belenky, G. Kipshidze, T. Hosoda, J. Chen, D. Wang, L. Shterengas, "GaSb-based laser operating within the spectra range of 2-3 μm," Advanced Workshop on Frontiers in Electronics (WOFE 09), December 13-16 (2009), Rincon, Puerto Rico.
8. T. Hosoda, G. Kipshidze, L. Shterengas, D. Westerfeld, S. Suchalkin, G. Belenky, "3 μm Type-I GaSb-based diode lasers operating at room temperature in CW mode," 26th North American Molecular Beam Epitaxy Conference (NAMBE), August 9-12 (2009), Princeton, NJ.
9. G. Belenky, L. Shterengas, G. Kipshidze, T. Hosoda, J. Chen, S. Suchalkin, "GaSb-based Laser diodes operating within spectral range of 2-3.5 μm," Conference on Lasers and Electro-Optics, 2009 (CLEO'09), May 31-June 5 (2009), Baltimore, MD.
10. G. Belenky, G. Kipshidze, L. Shterengas, D. Donetsky, T. Hosoda, J. Chen, S. Suchalkin, "GaSb based lasers operating within spectral range above 2 μm," SPIE Photonics West, January 24-29 (2009), San Jose, CA.